

# An optical spectroscopic based reflective sensor for CO<sub>2</sub> measurement with signal to noise ratio improvement

M. R. SALIM<sup>a</sup>, M. YAACOB<sup>b</sup>, M. H. IBRAHIM<sup>a</sup>, A. I. AZMI<sup>a</sup>, N. H. NGAJIKIN<sup>a</sup>, G. DOOLY<sup>c</sup>, E. LEWIS<sup>c</sup>

<sup>a</sup>Universiti Teknologi Malaysia, Faculty of Electrical Engineering, 81310 Skudai, Johor, Malaysia.

<sup>b</sup>Department of Communication Engineering, Universiti Tun Hussein Onn Malaysia, Batu Pahat, Johor, Malaysia

<sup>c</sup>University of Limerick, Department of Electronic and Computer Engineering, Plassey Road., Limerick, Ireland

This paper presents recent work in measuring carbon dioxide (CO<sub>2</sub>) using an absorption spectroscopy method within the mid-IR region. A multi-path optical fibre based reflective sensor is proven to be capable of detecting CO<sub>2</sub> at lower level (<15%) and higher level of concentration (>15%). For low level detection, the sensor is capable of measuring CO<sub>2</sub> concentration from 0.8% to 14.8%, while for high level of detection, the sensor showed its capability to detect CO<sub>2</sub> concentration from 15.1% to 44.6% with high accuracy. By eliminating unwanted noises using suitable filtering technique, the voltage response from the system has become more stable and without significant loss in voltage, thus improving the signal-to-noise ratio and stability of the system. The average signal-to-noise ratio for each of the filter types, no filter, lowpass, bandpass were calculated as being 53.4, 69.1 and 119.0 respectively. Similarly, moving average technique was developed in LabVIEW to improve voltage response with less noise and interference, resulting better overall system's performance.

(Received March 30, 2015; accepted May 7, 2015)

*Keywords:* Absorption spectroscopy, Mid-infrared, carbon dioxide, filtering, moving average technique

## 1. Introduction

It is well known since the early 1800's that various atmospheric gases act "like glass in a greenhouse" whereby they transmit incoming sunlight and absorb outgoing infrared radiation. This process can ultimately raise the average historical air temperature on the Earth's surface. Carbon dioxide (CO<sub>2</sub>) is one of the primary pollutant gases produced through the combustion of fossil fuels and has been recognized as being one of the most influential greenhouse gases. Over the past 420,000 years ago, the CO<sub>2</sub> content in the atmosphere has varied cyclically with a period of about 100,000 years (in conjunction with variations in the Earth's orbit) between a minimum value of about 180 parts-per-million by volume and a maximum of about 290 parts-per-million [1]. When the CO<sub>2</sub> level was still sitting at about 280 parts-per-million, or near the top of a very gradual geological cycle, the level however began to shoot upward in 1850. It has already reached the unprecedented value of 380 parts-per-million, 36% increase over the pre-industrial value and is continuously rising at the incredible rate of about 2 parts-per-million per year<sup>1</sup>.

These increases in atmospheric CO<sub>2</sub> levels can give rise to a process known as 'global warming' and can have detrimental effects on both human and animal life here on earth<sup>2</sup>. One of the primary sources of these atmospheric gases comes from the emission of CO<sub>2</sub> gases during the use of internal combustion engines and can lead to large scale releases of CO<sub>2</sub> into the Earth's atmosphere on a daily basis. The basic automotive combustion engine producing on average, roughly, 2% CO<sub>2</sub> while in operation, however many varieties of engines exist<sup>3</sup>. The

need for a sensor, capable of monitoring CO<sub>2</sub> emissions can have vast applications within industrial, private and commercial enterprises worldwide.

There are various spectroscopy techniques adopted in optical fibre sensors nowadays to measure and monitor the level of gas concentration. Optical spectroscopy techniques offer direct, rapid, and often highly selective means of accurately measuring gas concentration<sup>4</sup>. However, to use spectroscopy technique, the gas detected must have significant distinct absorption, emission or scattering in a convenient region of the optical spectrum<sup>5</sup>. Figure 1 illustrates optical spectrum of absorption cross section in mid-infrared region for various atmospheric gases such as carbon dioxide (CO<sub>2</sub>), carbon monoxide (CO), sulphur dioxide (SO<sub>2</sub>), nitrogen dioxide (NO<sub>2</sub>) & water vapour (H<sub>2</sub>O) at ambient pressure and temperature. Optical fibre sensors operating in the UV and near-infrared region of the electromagnetic spectrum for the detection of gases such as SO<sub>2</sub>, NO<sub>2</sub>, nitric oxide (NO) and ammonia (NH<sub>3</sub>) have been reported previously<sup>6-8</sup>. In addition to this, highly sensitive mid-infrared optical fibre sensors using absorption spectroscopy have also been developed for the detection of CO<sub>2</sub><sup>9-11</sup> and CO<sub>12</sub> within exhaust emissions. These have been developed for both transmissive<sup>7,9,13</sup> and reflective techniques<sup>10,14</sup>.

Previous researchers have proved their CO<sub>2</sub> gas sensors work effectively and are capable of detecting CO<sub>2</sub> gas over a wide range of concentrations with fast response times. However, the lowest CO<sub>2</sub> gas concentration that could be detected was approximately reported to be 1% with response times shown to be in the order of milliseconds<sup>10,14</sup>. In contrast, there are reported different configurations of CO<sub>2</sub> gas detection in.

which covering much smaller level of concentration but suffer higher response times. For instance, more than 40 seconds and up to 10 seconds of response times recorded for the concentration detection of as low as 0.05%<sup>15</sup> and 0.001%<sup>16</sup> respectively. In comparison to previous measurement with similar configuration applied<sup>10,14</sup>, although our recorded recovery times appear relatively slow, this was due to the small flow rates used during measurement, resulting in slow purging of the gas cell and CO<sub>2</sub> gas molecules remaining in the gas cell for a slightly extended period of time. However, we successfully managed to develop an optical fibre based sensing system for CO<sub>2</sub> gas measurement that capable of detecting lower

level of CO<sub>2</sub> gas concentration as low as 0.8%. It has shown that our optical fibre based reflective sensor is adequately reliable and competitive in measuring CO<sub>2</sub> gas concentration. We have adopted rigorous techniques such as filtering technique<sup>17</sup> and moving average technique<sup>18</sup> in order to decrease the influence of noise and interference, subsequently resulting in better output response and signal-to-noise ratios (discussed further in Section 3). Both techniques were essentially applied to the developed comprehensive LabVIEW program in order to get smoother voltage response in which can further enhance the results achieved.

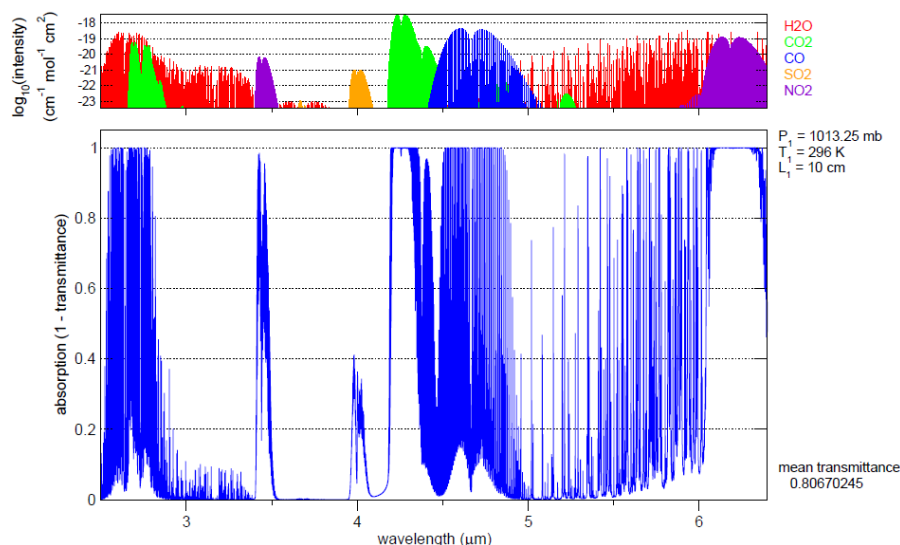


Fig. 1. Above - absorption Cross Section for various atmospheric gases in Mid-Infrared region; Below – summation of all absorbing species (H<sub>2</sub>O, CO<sub>2</sub>, CO, SO<sub>2</sub>, NO<sub>2</sub>) within the Mid-Infrared region<sup>5</sup>

## 2. Theory

Generally, different gas molecules will absorb radiation at different wavelengths, as each gas species has their own individual absorption spectrum<sup>9,10</sup>. For example, two gases, namely SO<sub>2</sub> and NO, both have characteristic strong absorption lines in the ultraviolet region but weaker mid-infrared overtones absorption peaks at 4 μm and 5.3 μm respectively. On the other hand, CO<sub>2</sub> has a characteristically strong absorption band in the mid-infrared region, extending from 4.2 μm to 4.5 μm, with its high peaks at 4.23 μm and 4.28 μm wavelengths. Apart from that, CO<sub>2</sub> also shows a weaker corresponding near-infrared overtones absorption band around 2.7 μm, two orders of magnitude lower than that at 4.28 μm wavelength as shown in Fig. 1.

The linear relationship between absorption and concentration of an absorbing species can easily be calculated by using the Beer-Lambert law, which is shown in equation (1). It is most commonly used to calculate how much incident radiation is absorbed by a sample. This is described in detail by many chemistry textbooks and journals<sup>19</sup>:

$$\frac{I_t}{I_o} = e^{-(\epsilon \times c \times l)} \quad (1)$$

Where  $I_t$  is the transmitted intensity or the radiation after absorption,  $I_o$  is the incident intensity or the radiation before absorption,  $\epsilon$  ( $\text{cm}^2/\text{mol}$ ) is the wavelength dependent molar absorptivity of the species,  $l$  ( $\text{cm}$ ) is the optical path length and  $c$  ( $\text{mol}/\text{cm}^3$ ) is the concentration of the absorbing species.

A variation of the Beer-Lambert Law was utilized by a specifically designed LabVIEW program to calculate the concentration of the gases present. The concentration of the species and molar absorptivity of the species can also be expressed in different terms as shown as follows:

$$\epsilon = \sigma \times N_A \quad (2)$$

$$c = \frac{\phi \times d}{w \times 10^6} \quad (3)$$

Where  $\sigma$  ( $cm^2/Molecule$ ) is the wavelength dependent absorption cross section of the species,  $w$  ( $kg/mol$ ) is the molecular weight of the species,  $d$  ( $kg/cm^3$ ) is of the density of the species in air by volume,  $N_A$  ( $Molecule/mol$ ) is Avogadro's constant and  $\phi$  (arb.) is the parts-per-million of CO<sub>2</sub>, or ratio of CO<sub>2</sub> molecules to total molecules, in the atmosphere. Hence, substituting (2) & (3) into (1) will give:

$$\frac{I_t}{I_o} = e^{-(\sigma \times N_A) \times \left[ \frac{\phi \times d}{w \times 10^6} \right] \times l} \quad (4)$$

Therefore,

$$\phi = \frac{-\left[ \ln \frac{I_t}{I_o} \right] \times w \times 10^6}{\sigma \times N_A \times d \times l} \quad (5)$$

or,

$$\sigma = \frac{-\left[ \ln \frac{I_t}{I_o} \right] \times w \times 10^6}{\phi \times N_A \times d \times l} \quad (6)$$

The signal strength received from each of the pyroelectric detectors was recorded before and after the gas was allowed into the gas chamber. A variation of equation (5) shown in equation (6) was utilized to calculate the measured absorption cross section for CO<sub>2</sub>. This measured absorption cross section represents the average of the absorption present across the full spectrum of the filter range (discussed further in Section 4). This

value will be used during further tests to calculate the concentrations of CO<sub>2</sub> present in the gas chamber.

### 3. Proposed Technique

Instead of using transmissive type for gas chamber, we chose to use reflective type. In comparison, a reflective gas cell is not only compact in size, but also offers better sensitivity due to its longer optical light path. It is proven from Beer-Lambert law in which absorption is directly dependent on path length of the gas cell<sup>19</sup>. Initially, the pulsed infrared radiation from the emitter was launched from the transmitting optical fibre into the measurement chamber using a collimating lens. Following transmission into the gas chamber, the infrared radiation traveled across 18.5 mm of the open space where it interacted with the measurand gas before coming in contact with a perpendicular aluminium end surface. Upon contact with the aluminium surface, parts of the infrared radiation was transmitted back to the same collimating lens where it was condensed onto the end of the receiving optical fibre. Hence, the infrared radiation would have to propagate twice in the gas chamber to reach the receiving fibre. This has indirectly doubled the total of optical path length, subsequently resulting in better sensitivity.

Filtering technique was used in such a way that the recorded output voltage response has less noise<sup>17</sup>. It is essential to ensure that our signal data is free from the influence of interference. Initially, few measurements such as using Low Pass filter and Bandpass filter with different orders and cut off frequencies were tested to determine the best filter type that could be used for this filtering technique. Some of these experimental results are repeated in Fig. 2 below.

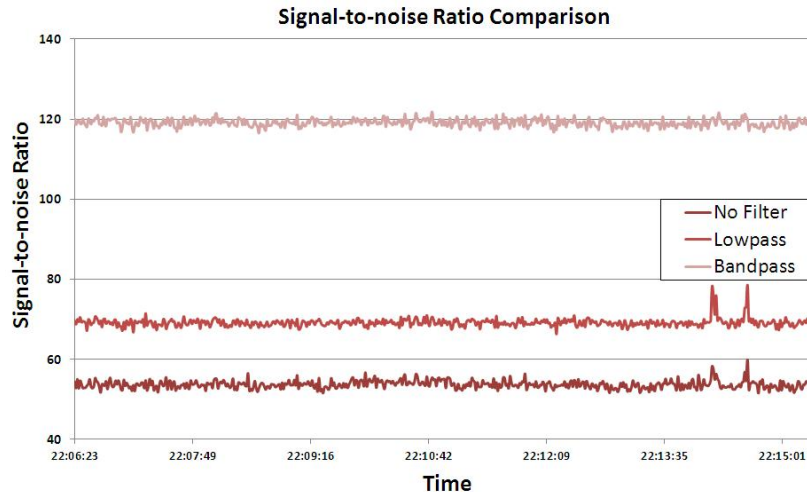


Fig. 2 Comparison of signal-to-noise ratio for several digital filter topologies employed during initial experimental tests

Fig.2 shows recorded results from an experimental test employing three digital filter types simultaneously, specifically no filtering, a first-order lowpass with 2.5Hz cutoff and sampling frequency of 1000Hz, and a first-order bandpass with a lower cutoff of 1.5Hz, higher cutoff of

2.5Hz and sampling frequency of 1000Hz. The raw voltage readings were recorded while nitrogen was present within the gas cell for a total of 10 minutes and then passed through each of the filters within a LabVIEW VI. Each

data set was then used to calculate the signal to noise ratio over time, as shown in Fig. 2, using equation 7<sup>20</sup>.

$$SNR = \mu / \delta \quad (7)$$

Where  $SNR$  (*arb.*) is the signal-to-noise-ratio (level of a desired signal to the level of background noise),  $\mu$  (*volts*) is the signal mean or expected value and  $\delta$  (*volts*) is the standard deviation of the noise taken from the full dataset<sup>20</sup>.

The results shown in Fig. 2 clearly show a marked improvement in the response from the sensing system. The average signal-to-noise ratio for each of the filter types, no filter, lowpass, bandpass were calculated as being 53.4, 69.1 and 119.0 respectively. By eliminating unwanted noise the voltage response from the system has become more stable and without significant loss in voltage, thus increasing the signal-to-noise level and stability of the system.

For this purpose, we chose first order of Bandpass filter with 2.5 Hz and 1.5 Hz for high cut off frequency and low cut off frequency respectively and the sampling frequency was set to be 1000 Hz. The recorded voltage signal by using Bandpass filter above has experimentally proven to be more stable and have much higher signal-to-noise ratio than others. Hence, the filtering result for this filter's specification chosen is much better in terms of the voltage response as compared to other types of filter topologies for this experiment set-up.

Moving average technique was adopted in this measurement to get smoother voltage signal with less noise and interference<sup>18</sup>. It is known that the higher number of points we choose, the smoother graph output will be obtained. However, too high number of points used in this technique will affect the overall response time. Although a lower noise can be achieved by having the

higher number of averaged points, the resultant delay of the actual measured value has to be tolerated. In this experiment, we set 10 points for double moving average process with time interval between points was set to be in the order of milliseconds. We developed the moving average technique in LabVIEW program after filtering technique implemented where the amplitude of the filtered voltage responses were transferred to the averaging section.

#### 4. Experimental Set-Up

The experimental set-up of the optical-fibre-based reflective sensor system as assembled in the laboratory is shown in Fig. 3. The developed optical fibre sensor using low cost and compact mid-infrared region component, consists of a broadband infrared radiation light source (2.0 to 8.0  $\mu\text{m}$ ) from filament emitter NL5LNC pulsable (0.5–10 Hz) nichrome from ion optics, 50 mm in length-infrared 4-to-1 fibre bundle from Art Photonics<sup>21</sup>, two LME 335 pyroelectric detectors<sup>22</sup>, and also a reflective gas cell where flat aluminium reflective surface was used at the end of one side of the gas cell while single lens located at the other side. The fibre bundle consisted of the same 500/550  $\mu\text{m}$  multimode, core/clad, Chalcogenide InfraRed fibre ( $\text{As}_2\text{S}_3$ -based material) and was capable of low attenuation at wavelengths close to 4.25  $\mu\text{m}$ <sup>21</sup>. The pyroelectric detectors are fitted with two different filters, one with Narrow Bandpass filter (center frequency at 4.26  $\mu\text{m}$ ) for  $\text{CO}_2$  detection and the other with a reference filter at a centre wavelength of 3.95  $\mu\text{m}$ <sup>22</sup>. Note that the detection method for this experiment set-up is pyroelectric detectors with narrowband filter in which measuring the average of the absorption present across the full spectrum of the filter range (range being 180nm).

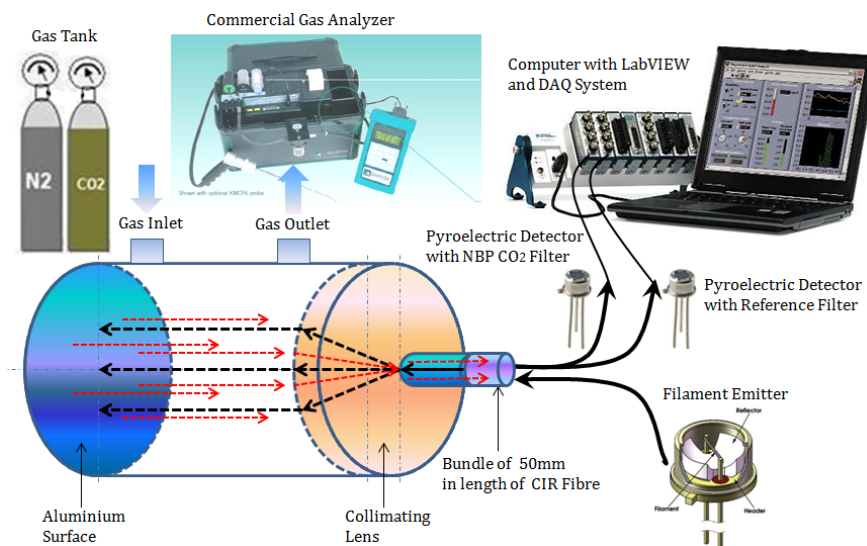


Fig. 3 Mid-infrared optical fibre based reflective sensor

The voltage response of the sensor was detected by a computer by using a National Instruments BNC 2110 data acquisition (DAQ) card and LabVIEW software. A specifically designed LabVIEW program has been developed for use in the sensing system as a means of controlling data acquisition from the receiver circuitry and also data output to the user. A commercial Quintox flue gas analyzer was used simultaneously in the experimental set-up in order to provide a comparison reading of the concentration of carbon dioxide gas present in the gas mixing chamber.

## 5. Results and Discussion

Initial calibration of the reflective based sensor using the commercial Quintox flue gas analyzer was required in order to ensure that the sensor is really capable of generating accurate concentration readings. For this purpose the average absorption cross section for CO<sub>2</sub> needed to be measured. This measured absorption cross section represents the average absorption cross section for CO<sub>2</sub> covered by the narrow bandpass filter in the wavelength range 4.14  $\mu\text{m}$  and 4.32  $\mu\text{m}$ <sup>22</sup>. Laboratory based experiments were carried out using the experimental set-up described earlier. The CO<sub>2</sub> gas was released at a constant concentration and the commercial Quintox flue gas analyzer accurately recorded the concentration of the gas under test. The output signals received from each of the pyroelectric detectors were recorded before and after the measurand gas was released into the gas cell. This data was used in equation 6 to calculate the measured value which in turn was then hard-coded into the LabVIEW VI, completing the calibration process.

Following completion of the calibration process a number of varying concentration gas tests were carried out in order to fully quantify the capability of the sensing system. For this the commercial Quintox flue gas analyzer, used to run a simultaneous measurement, provided reliable and accurate readings of the concentrations present in the gas chamber. The concentration of the gases present can therefore be calculated using equation 5 with all other factors known. All the required factors are accessible during testing and therefore LabVIEW program was specifically developed (discussed previously in Section 2) to access this data and output the CO<sub>2</sub> concentration to the user in real time.

Fig. 4 illustrates the voltage signal response for 2 cycles CO<sub>2</sub> Standard measurement showing the reading of averaged concentration from optical sensor and measured concentration from commercial Quintox flue gas analyzer at every stage over wide range of concentration. From the graph, it is proven that the sensor is capable of detecting various levels of CO<sub>2</sub> concentrations (shown as percentage – 1% equals 10,000 parts-per-million). The graph also mainly indicates the difference between response with moving average and without moving average techniques. The graph proves that our sensor are capable of detecting CO<sub>2</sub> concentration between 0.8% and 14.8% for first cycle

while CO<sub>2</sub> concentration between 0.6% and 11.8% for the following cycle as measured by Quintox analyzer. However there is a noticeable shift in the voltage peaks between each of the cycles, this may be due to temperature changes in the heating of the filament emitter and needs further investigation.

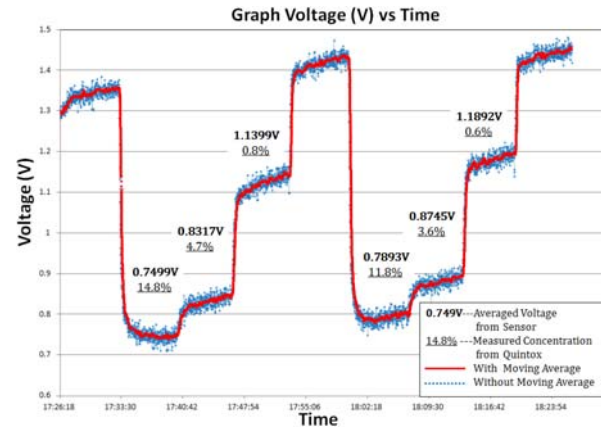


Fig. 4 CO<sub>2</sub> standard voltage response for 2 cycles measurement

Voltage output for CO<sub>2</sub> long measurement is illustrated in Fig. 5. This experiment entailed using a slightly higher wavelength Narrow Bandpass filter (center frequency at 4.45  $\mu\text{m}$ ) mounted onto the detector, allowing for lower sensitivity and higher detection range<sup>22</sup>. This measurement was specifically carried out for higher level of gas concentration starting from 15%. From the graph, it proved the capability of the sensor to detect higher level of concentration from 15% and up to 45%. Obviously, as the CO<sub>2</sub> concentration is decreased, the voltage reading is increased.

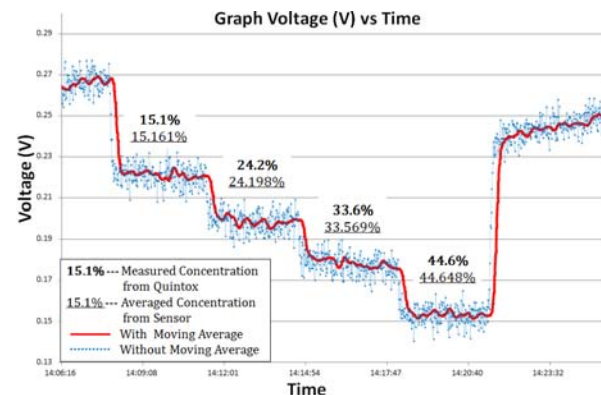


Fig. 5 CO<sub>2</sub> long voltage response with respective CO<sub>2</sub> concentration

The average value of all the measured voltage points when there was no gas is recorded to be 0.2659V. The averaged voltage reading for 15.1% CO<sub>2</sub> concentration step is recorded to be 0.2221V and followed by 0.1995V, 0.1785V and 0.1565V for CO<sub>2</sub> concentration of 24.2%,

33.6% and 44.6% respectively. From Fig. 5, it is clear that the averaged concentration recorded by the sensor during the measurement is accurate and seems to agree well with the readings from the Quintox flue gas analyzer. Moving average process adopted using 10 points for twice and the steps changed for every 200 seconds.

Recorded Rise Time and Fall Time for voltage output response are then analyzed as illustrated in Fig. 6(a) and (b). It is noticeably the recorded Rise Time is similar to Fall Time where 26 seconds and 30 seconds for rise time and fall time using a 20 point average were recorded respectively. Although these response and recovery times are relatively large when compared to that of the non-averaged data, the times are sufficient for monitoring purposes and are comparable to many commercial sensors. It shows that the developed optical sensor is very responsive and has capability of detecting the CO<sub>2</sub> promptly. Significant affect of 20 points moving average and filtering techniques applied during measurement carried out are clearly shown on the graphs for comparison.

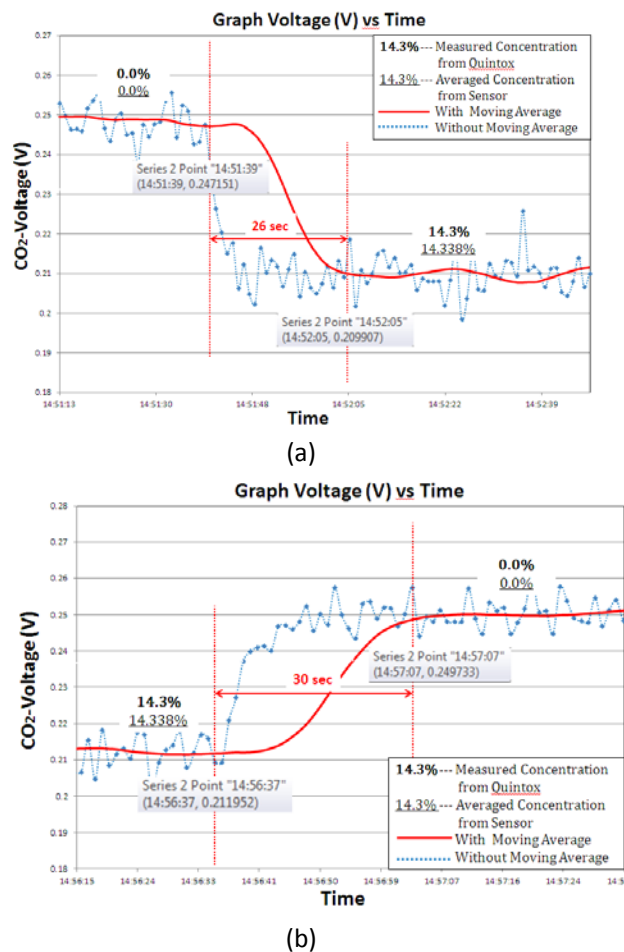


Fig. 6 Zoomed voltage response for CO<sub>2</sub> long measurement: (a) rise time and (b) fall time

## 6. Conclusion

A multi-path optical fibre based reflective sensor has been successfully developed. The sensor has shown a good dynamic range of CO<sub>2</sub> gas detection since it has the capability of accurately detecting two different ranges of CO<sub>2</sub> concentration; below 15% and above 15%. For lower level of CO<sub>2</sub> concentration measurement, the sensor has shown that it was able to capture voltage for CO<sub>2</sub> concentration from 0.8% to 14.8% for first cycle of measurement followed by from 0.6% to 11.8% for the following cycle of measurement. In short, for CO<sub>2</sub> standard measurement, the sensor is capable of detecting the CO<sub>2</sub> concentration as low as 0.6% and up to 14.8%.

Meanwhile, CO<sub>2</sub> long measurement for CO<sub>2</sub> concentration greater than 15% was recorded starting from 15.1% to 44.6% of concentration where the measured concentration results agreed closely to that of the commercial gas analyzer.

CO<sub>2</sub> measurement was carried out for two ranges of concentration for this work. The first level of concentration is below 15% namely CO<sub>2</sub> Standard measurement while higher level of CO<sub>2</sub> concentration namely CO<sub>2</sub> Long measurement was set to be greater than 15%. For both ranges of concentration, we are able to prove the capability and reliability of the sensor with better response time. The sensing system developed is proven to be very responsive and has capable response times, 26 seconds and 30 seconds for rise time and fall time respectively.

Filtering technique and moving average technique were adopted as an ongoing process resulting in better output response. Due to the significant effect on the output responses, our sensor has been experimentally proven to be highly responsive and has the ability of accurately detecting CO<sub>2</sub> gas concentration varied during measurement. Future work will concentrate on designing the optimum and low cost structure of gas chamber by replacing the flat aluminum used with the various types of reflective surfaces (eg. sphere, ellipse, hyperbola, parabolic) and by replacing collimating lens with lower cost component such as CaF<sub>2</sub> windows.

## Acknowledgments

The authors would like to thank the staff of the Electronic and Computer Engineering Department of the University of Limerick, Ireland for their continued assistance during testing and measurement. The authors would also like to acknowledge the support of the Human Capital Development, Universiti Teknologi Malaysia, Malaysia for funding this research.

## References

- [1] C. Kutscher, Automotive emissions and the greenhouse effect, July/August 2006 issue of SOLAR Today magazine.
- [2] James Hansen, A Climate Change, **68**, 269 (2005).
- [3] P. A. Vesilind, Environmental Pollution and Control, 3rd ed., Butterworth-Heinemann, 1990, pp. 241–251.
- [4] P. Chambers, A Study of a Correlation Spectroscopy Gas Detection Method, Thesis 2005
- [5] Spectral Calc.com, High Resolution Spectral Modeling, by GATS, Inc., <http://www.spectralcalc.com/info/about.php>
- [6] A. Fateev, S Clausen, Source: International Journal of Thermophysics, **30**(1), 265 (2009).
- [7] G. Dooly, E Lewis, C. Fitzpatrick, P. Chambers, Source: IEEE Sensors Journal **7**(5), 685 (2007).
- [8] A. Sansubrin, M. Mascini, Source: Biosensors and Bioelectronics, **9**(3), 207 (1994).
- [9] J. Mulrooney, J. Clifford, C. Fitzpatrick, P. Chambers, E. Lewis, Journal of Optics A: Pure and Applied Optics, **9**(6), S87 (2007).
- [10] R. Muda, G. Dooly, J. Clifford, J. Mulrooney, G. Flavia, E. Merlone-Borla, P. Chambers, C. Fitzpatrick, E. Lewis, Journal of Optics A: Pure and Applied Optics, **11**(5), (2009).
- [11] F. Charpentier, J. Troles, Q. Coulombier, L. Brilland, P. Houizot, F. Smektala, C. Boussard-Pledel, V. Nazabal, N. Thibaud, K. Le Pierres, Renversez; Bureau, B. Source: Sensor Letters, **7**(5), 745 (2009).
- [12] Eva S. Norris, Nic Chormaic, G. Sile Source: Proceedings of SPIE - The International Society for Optical Engineering, **4876**(2), 923 (2002).
- [13] Zhang, Guangjun; Li, Yaping; Li, Qingbo, Optics and Lasers in Engineering, **48**(12), 1206 (2010).
- [14] Dooly, Gerard; Mulrooney, Jim; Merlone-Borla, Edoardo; Flavia, Gili; Clifford, John; Fitzpatrick, Colin; Lewis, Conference Record - IEEE Instrumentation and Measurement Technology Conference, p 1891-1894, 2008, 2008 IEEE International Instrumentation and Measurement Technology Conference Proceedings, I2MTC.
- [15] Bhande, Sambhaji S. Mane, Rajaram S.; Ghule, Anil V.; Han, Sung-Hwan, Scripta Materialia, **65**(12), 1081 (2011).
- [16] Yoon, Hyeun Joong; Jun, Do Han; Yang, Jin Ho; Zhou, Zhixian; Yang, Sang Sik; Cheng, Mark Ming-Cheng, Sensors and Actuators, B: Chemical, **157**(1), 310 (2011).
- [17] Smith, Steven; Digital Signal Processing: A Practical Guide for Engineers and Scientists, Page 6, ISBN-13: 9780750674447, Elsevier Newnes, 2002.
- [18] He, Jimin; Fu, Zhi-Fang; Mathematics for modal analysis, ISBN-13: 9780750650793, Butterworth-Heinemann, 2001.
- [19] P. Fernando and G. Ernesto, Spectrochimica Acta Part A, **59**, 1223 (2003).
- [20] J. T., Bushberg, et al., The Essential Physics of Medical Imaging, (2e). Philadelphia: Lippincott Williams & Wilkins, 2006, p. 280.
- [21] Database reference and server website, Hisky website page for Art Photonics CIR Fibre <http://www.hisky-hk.com/images/201104/1303378867PDF89598.pdf>
- [22] InfraTec; <http://www.infratec.eu/>

---

\*Corresponding author: rashidi@fke.utm.my